applied sciences

MDPI

*Article*

# Screening Additives for Amending Compacted Clay Covers to Enhance Diffusion Barrier Properties and Moisture Retention Performance

**Min Wang [1], Jiaming Wen [2], Heng Zhuang [1], Weiyi Xia [3], Ningjun Jiang [1] and Yanjun Du [1,*]**

1 Jiangsu Key Laboratory of Urban Underground Engineering & Environmental Safety, Institute of Geotechnical Engineering, Southeast University, Nanjing 210096, China; wang-min@seu.edu.cn (M.W.); zhuangheng@seu.edu.cn (H.Z.); jiangn@seu.edu.cn (N.J.)
2 Zijin (Changsha) Engineering Technology Co., Ltd., Changsha 410006, China; wenjiaming@seu.edu.cn
3 Jiangsu Environmental Engineering Technology Co., Ltd., Nanjing 210019, China; xiaweiyi@seu.edu.cn
* Correspondence: duyanjun@seu.edu.cn

**Featured Application: The dual-additives-amended compacted clay covers in this article could apply to the cover system of industrial contaminated sites, municipal solid waste landfill, and industrial solid waste landfill. The dual-additives could enhance the anti-cracking, moisture retention, gas barrier, and hydraulic performance of compacted clay covers.**

**Abstract:** The cover systems in contaminated sites have some problems, including desiccation cracks, which would lead to degradation of the barrier performance. This study presented a systemic laboratory experimental investigation on the liquid–plastic limit, moisture retention, hydraulic conductivity ($k$), and gas diffusion barrier properties of amended compacted clay by attapulgite and diatomite for controlling desiccation cracks and migration of water and volatile organic compounds (VOCs). The results showed that the attapulgite could enhance the moisture retention and liquid limit of amended compacted clay. Diatomite could reduce the gas diffusion coefficient ($D_\theta$) significantly. The compacted clay amended by the dual-additives component of attapulgite and diatomite could enhance the liquid limit, moisture retention percent, gas barrier property, and hydraulic performance compared with the unamended clay. Based on the experimental data obtained, the dosage of additives was targeted to be 5%. The moisture retention percent of dual-additives (attapulgite 4% and diatomite 1%) amended clay increased by 82%, the $k$ decreased by 25%, and the $D_\theta$ decreased by 42% compared with unamended clay. Scanning electron microscopy (SEM), BET-specific surface area test method (BET), Mercury Intrusion Porosimetry (MIP), and thermogravimetric analysis (TGA) indicated the enhancement mechanism of additives-amended compacted clay.

**Keywords:** additives; compacted clay cover; moisture retention; gas diffusion barrier; hydraulic conductivity

check for updates

**Citation:** Wang, M.; Wen, J.; Zhuang, H.; Xia, W.; Jiang, N.; Du, Y. Screening Additives for Amending Compacted Clay Covers to Enhance Diffusion Barrier Properties and Moisture Retention Performance. *Appl. Sci.* **2022**, *12*, 7341. https://doi.org/10.3390/app12147341

Academic Editor: Bing Bai

Received: 9 June 2022
Accepted: 18 July 2022
Published: 21 July 2022



## 1. Introduction

The cover system, including compacted clay cover (CCC) and geomembrane (GM), applied in contaminated sites could prevent the migration of volatile or semi-volatile organic compounds (VOCs/SVOCs) and limit the movement of precipitation into the underlying waste [1–5]. However, the published literature [6–8] have shown that the cover system has some problems, including geomembrane defects, and desiccation cracks of the CCC, which would lead to the degradation of the barrier performance (Figure 1). Rowe et al. [6] presented that the geomembrane defects are inevitable. The monitoring results of 205 sites show that the percent of complete geomembrane is less than 30%. In addition, more than 50 percent of geomembranes have more than five loopholes per ha. The barrier performance of the cover system would be degraded by geomembrane defects. Then, the CCC contributes to the role of VOCs/SVOCs and the precipitation barrier. However, desiccation cracks in CCC act as preferential flow paths and affect the barrier performance of CCC, eventually breaking through the cover system [9]. There are various issues resulting in cracks of CCC [7,10], including differential settlements, extreme drought [11], and dry–wet cycle [9]. The resistance to cracking, i.e., the tensile strength or fracture toughness of the soil, also changes upon drying. Finally, the adhesion at interfaces, which is essential in providing the restraint for desiccation cracks to form, changes with moisture content [12,13]. Omidi et al. [8] showed that the hydraulic conductivity increases nearly two orders of magnitude due to the desiccation cracks of CCC, which would have a great impact on the cover system. Albrecht and Benson [14] presented that the hydraulic conductivity of cracked soils is typically several orders of magnitude greater than that of intact soils.

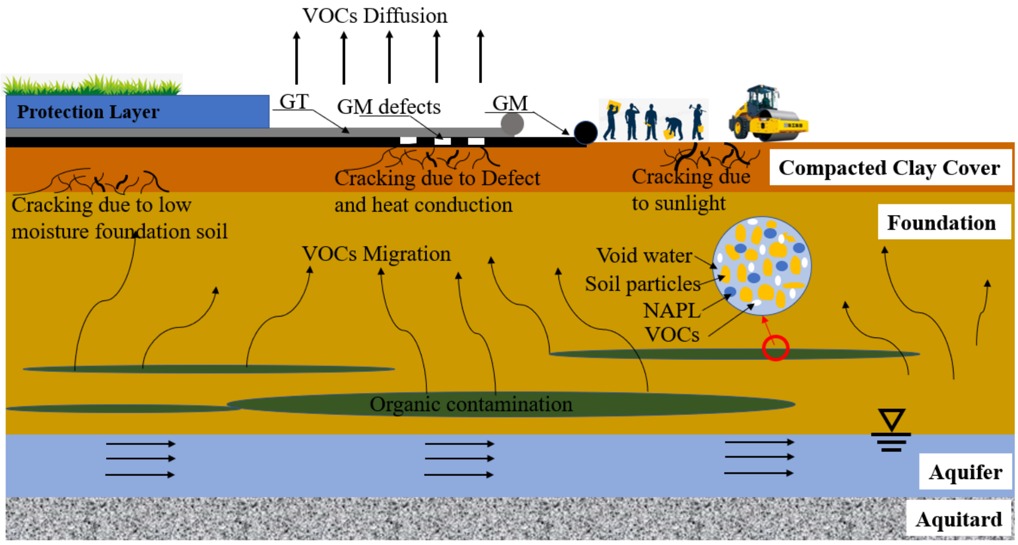


**Figure 1.** Problems of compacted clay cover desiccation and possible migration of VOCs [6–14].

To restrain the desiccation cracks of CCC, moisture retention additives were added to the soil to improve its moisture retention and desiccation cracks inhibition performance. Moisture retention additives could inhibit moisture evaporation and regulate soil temperature by adsorbing water hundreds or even thousands of times its weight [15]. According to different synthetic materials, the moisture retention additives can be divided into four kinds: modified starch, synthetic polymer, modified cellulose, and other natural compounds and their derivatives, blends, and composites [16]. It is cumbersome to prepare the synthetic polymer moisture retention additives. In addition, it is not suitable for practical engineering because the synthetic polymer would be completely degraded in soil within some years [17]. Therefore, natural materials and their derivatives could be selected as amended materials, namely attapulgite, diatomite, and zeolite. However, the natural zeolite cannot meet the requirements due to its small pore size and being easy to block [18]. Finally, attapulgite and diatomite are proposed as additives for amending CCC.

Usually, the migration modes of gases in the soil included advection and diffusion [5]. Conant et al. [19] found that diffusion is the main migration mode of trichloroethylene (TCE) vapor through a detailed, field-scale analysis of the transport behavior of solvent vapors within the unsaturated zone. The unsaturated zone at the site is approximately 3.5 m thick and comprises the upper portion of the sequence of glaciolacustrine sands and silts of the Borden aquifer. You et al. [20] found that although the transient advective flux can be greater than the diffusive flux; under most of the field conditions the net contribution of the advective flux is one to three orders of magnitude less than the diffusive flux. The advective flux contributes comparably with the diffusive flux only when the gas-filled porosity is less than 0.05. The advective transport of VOCs can be induced by the discrepancy in density between gas phase VOCs and clean air [21–23], water table fluctuation at coastal sites [21,23–25], and atmospheric pressure fluctuation [26,27]. Therefore, in most non-coastal sites and unsaturated zones with low permeability, the VOCs' migration mode in the organic contaminated sites is mainly diffusion [28–30]. Rowe [31] found that the gas barrier should not only prevent water migration, but also the organic contaminants transmission. Therefore, the development of amended CCC with excellent moisture retention and VOCs/SVOCs diffusion barrier performance is significant.

A systematic study of the moisture retention, hydraulic conductivity, and gas barrier properties of amended CCC was investigated through laboratory experiments. In this paper, the optimal dosage and ratio of dual-additives of the amended CCC were studied through the laboratory test. The hydraulic conductivity and gas barrier properties of amended CCC with optimal dosage and ratio were evaluated. Then, the mechanism behind the phenomenon was demonstrated through SEM, BET, MIP, and TGA test analyses.

## 2. Materials and Methods

### 2.1. Preparation of Amended Compacted Clay

Three types of amended compacted clay were prepared in this study: (1) the compacted clay amended by attapulgite with the dosage of 0%, 1%, 3%, 5%, and 10% (dry weight of attapulgite to dry weight of mixture powder); (2) the compacted clay amended by diatomite with the dosage of 0%, 1%, 3%, 5%, and 10% (dry weight of attapulgite to dry weight of mixture powder); and (3) the compacted clay amended by attapulgite and diatomite, here referred to as dual-additives, with the ratio of 4, 2, 1, 0.5, and 0.25 (dry weight of attapulgite to dry weight of diatomite); the dosage of dual-additives was attapulgite 4% and diatomite 1%, attapulgite 3.3% and diatomite 1.7%, attapulgite 2.5% and diatomite 2.5%, attapulgite 1.7% and diatomite 3.3%, and attapulgite 1% and diatomite 4% (dry weight of dual-additives to dry weight of mixture powder). The powdered clay used was obtained from Jining (Shandong, China), the powdered attapulgite and diatomite were manufactured by Zhengzhou (Henan, China). The optimum moisture content ($w_{op}$) and maximum dry density ($p_{dmax}$) were obtained by compaction test as per JTG E40 T0131-2007. This laboratory compaction method was used to determine the compaction curve compacted in a 152 mm diameter mold with a 45 N rammer dropped from a height of 450 mm, producing a compactive effort of 2677 kN-m/m$^3$ with 3 layers and 98 blows per layer. While, the ASTM D1557 compaction method was used to determine the compaction curve compacted in a 152.4 mm diameter mold with a 44.48 N rammer dropped from a height of 457.2 mm, producing a compactive effort of 2700 kN-m/m$^3$ with 5 layers and 56 blows per layer. The compaction curve of clay and dual-additives (attapulgite 4% and diatomite 1%)-amended clay are shown in Figure 2. The physical properties and main oxide content of these constituent materials used to prepare amended compacted clay are shown in Tables 1 and 2, respectively. The powdered materials used in this study were air dried and passed through a No. 200 (0.075 mm) sieve as specified in ASTM D 698 [32]. The initial moisture content of the specimens was determined to be 30% (weight of water to dry weight of solid). The liquid–plastic limit test and specific gravity test were conducted as per ASTM D 4318 [33] and ASTM D 854 [34], respectively, using distilled water.

**Table 1.** The physical properties of constituent materials used for preparing amended compacted clay.

| Property | Standard | Constituent Material | | |
|---|---|---|---|---|
| | | Clay | Attapulgite | Diatomite |
| Specific gravity, ($G_s$) | ASTM D854 (2014) | 2.73 | - | - |
| Liquid limit, *LL* (%) | ASTM D4318 (2018) | 54 | 197 | 121 |
| Plasticity index, *PI* (%) | | 26 | 105 | 35 |
| Classification | ASTM D2487 (2018) | CH | MH | MH |
| Optimum moisture content, $w_{op}$ (%) | JTG E40 T0131-2007 | 27.6 | - | - |
| Maximum dry density, $p_{dmax}$ (g/cm$^3$) | | 1.7 | - | - |

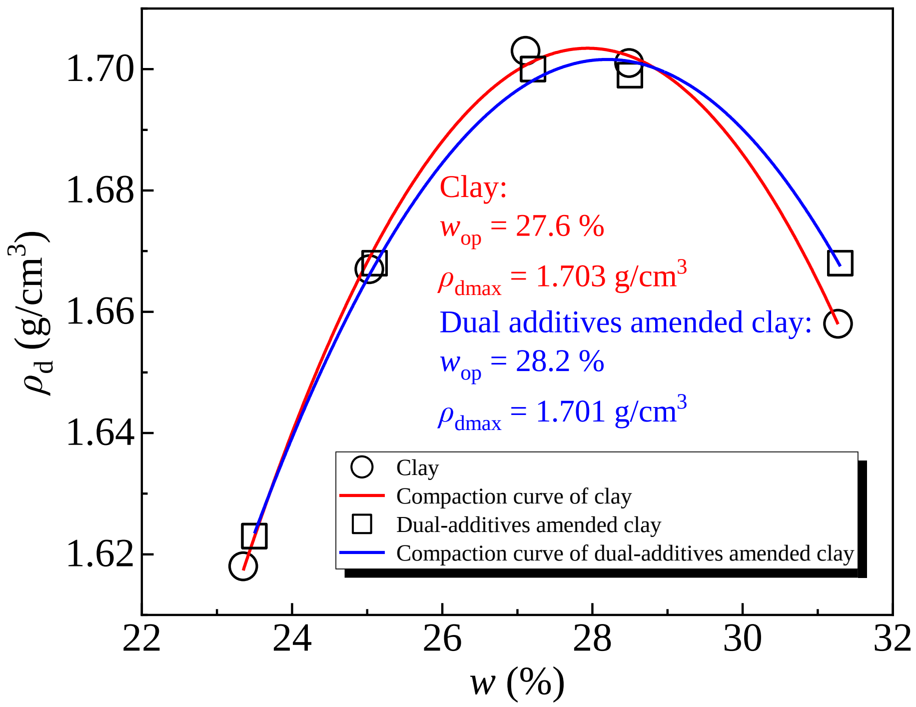


**Figure 2.** Compaction curve of the clay and dual-additives-amended clay.

**Table 2.** The main oxide content of attapulgite and diatomite.

| Component | | $SiO_2$ | $Al_2O_3$ | $Fe_2O_3$ | $Na_2O$ | $K_2O$ | CaO | MgO | MnO | $TiO_2$ | Loss |
|---|---|---|---|---|---|---|---|---|---|---|---|
| Content (%) | Attapulgite | 58.05 | 9.55 | 6.2 | 0.14 | 1.13 | 1.18 | 11.02 | 0. 61 | 0.47 | 11.65 |
| | Diatomite | 90.2 | 3.4 | 1.2 | 0.5 | 0.5 | 0.4 | 0.4 | 0. 61 | 0.2 | 2.59 |

The amended compacted clay in this study was prepared by mixing predetermined amounts of powdered clay, attapulgite, and diatomite directly. The dosage and ratio (dry weight basis) of additives are shown in Table 3. Then, the specimens were prepared by (1) mixing the air-dried clay, attapulgite, and diatomite thoroughly to prepare the dry mixture (Table 3); (2) adding predetermined amounts of tap water incrementally to the dry mixture, then mixing thoroughly and sealing for 24 h to assure homogeneity; (3) compacting by hydraulic pressure and sealing for 14 d until the specimens reached moisture balance. The number of parallel specimens was three. The coefficient of compaction was targeted to be 85%. The diameter of the specimens in the moisture retention and flexible-wall hydraulic conductivity test was set as 50 mm and the height was 50 mm. While, the diameter of the specimens in the gas diffusion test was set as 61.88 mm and the height was 20 mm.

**Table 3.** The experimental scheme of the moisture retention, liquid limit, and gas diffusion.

| Specimens | The Initial Moisture Content | The Additives Dosage | Ratio (Attapulgite: Diatomite) | Test Parameter |
|---|---|---|---|---|
| Attapulgite-amended | 30% | 0%, 1%, 3%, 5%, 10% | - | Moisture retention percent ($W_t$); Liquid limit ($LL$); Plastic limit ($PL$); Gas diffusion coefficient ($D_\theta$) |
| Diatomite-amended | | 0%, 1%, 3%, 5%, 10% | - | |
| Dual-additives-amended | | 5% | 4, 2, 1, 0.5, 0.25 | |

*2.2. Moisture Retention Test*

In the moisture retention test, the effects of attapulgite dosage, diatomite dosage, and dual-additives ratio on the moisture retention capacity of amended compacted clay were studied respectively. It was characterized by its moisture retention percent, as shown in Equation (1).

$$\mathrm{W_t} = \frac{\mathrm{m_{wt}}}{\mathrm{m_{w0}}} \cdot 100\% = \frac{\mathrm{m_s} \cdot \mathrm{w_0} - \mathrm{m_0} - \mathrm{m_t}}{\mathrm{m_s} \cdot \mathrm{w_0}} \cdot 100\% \quad (1)$$

where, $W_t$ is the moisture retention percent of the specimens at time $t$; $m_{wt}$ is the mass of moisture in the samples at time $t$; $\mathrm{m_{w0}}$ is the mass of moisture in the specimens at the initial time; $\mathrm{m_s}$ is the total mass of soil during specimens preparation; $\mathrm{w_0}$ is the initial moisture content during specimens preparation; $\mathrm{m_0}$ is the total mass of the specimens at the initial time; $m_t$ is the total mass of the specimens at time $t$.

The detailed test scheme of the moisture retention test is shown in Table 3. The dosage and ratio of dual-additives were determined through the orthogonal test. The test was conducted according to the following procedure: (1) placing the specimens in a 70 × 55 mm perforated aluminum box after sealing for 14 d; (2) placing the specimens in the oven, the temperature was targeted to be 60 °C, recording the mass change per three hours, and calculating the moisture retention percent of the specimens according to Equation (1) [35–38].

*2.3. Gas Diffusion Testing Procedures and Apparatus*

In the gas diffusion test, the effects of the attapulgite dosage, the diatomite dosage, and the ratio of dual-additives on the gas diffusion barrier performance of the amended compacted clay were conducted. Oxygen was used in this study, because when the gas dissolves easily in water or reacts with the components in the soil, the measured gas diffusion coefficient of the soil was low, resulting in the test error. The gas barrier performance of amended compacted clay was characterized by gas diffusion coefficient ($D_\theta$) per the research results of Taylor et al. [39–41]. $D_\theta$ was calculated based on the first Fick's law and the change rate of oxygen concentration in the diffusion chamber with time:

The first Fick's law is Equation (2):

$$\frac{\mathrm{d}q}{\mathrm{d}t} = -D_\theta \cdot \mathrm{A} \cdot \frac{\Delta C_t}{\mathrm{h_s}} \quad (2)$$

where: $q$ is the volume of gas diffusing into the chamber, $\mathrm{cm}^3$; $t$ is the diffusion time, s; A is the diffusion area of specimens, 30 $\mathrm{cm}^2$ in this study; $\mathrm{h_s}$ is the height of specimens, 2 cm in this study; $D_\theta$ is the gas diffusion coefficient of specimens, $\mathrm{cm}^2/\mathrm{s}$; $\Delta C_t$ is the gas concentration gradient of both ends of specimens, $\mathrm{g/cm}^3$.

The rate of gas diffusion volume into the chamber with time can be also presented as Equation (3):

$$\frac{\mathrm{d}q}{\mathrm{d}t} = \frac{\mathrm{d}(\Delta C_t)}{\mathrm{d}t} \cdot \mathrm{h_c} \cdot \mathrm{A'} \quad (3)$$

where: $\mathrm{h_c}$ is the height of the chamber, 15 cm in this study; A′ is the diffusion area of the chamber, 133 $\mathrm{cm}^2$ in this study.

Then, Equation (4) is obtained by combining Equations (2) and (3).

$$-D_\theta \cdot \mathrm{A} \cdot \frac{\Delta C_t}{\mathrm{h_s}} = \frac{\mathrm{d}(\Delta C_t)}{\mathrm{d}t} \cdot \mathrm{h_c} \cdot \mathrm{A'} \quad (4)$$

At the initial time ($t$ = 0), the oxygen concentration in the diffusion chamber is 0, in the atmosphere is $\mathrm{C_0}$, $\Delta \mathrm{C_0}$ was the difference between the oxygen concentration in the atmosphere and the diffusion chamber before the test, $\Delta \mathrm{C_0} = \mathrm{C_0}$. With initial conditions $t = 0$, $\Delta C_t = \Delta C_0 = C_0$, Equation (4) is integrated from 0 to $t$, obtaining results as Equation (5):

$$\ln\left(\frac{\Delta C_t}{\Delta C_0}\right) = -\frac{D_\theta}{h_s \cdot h_c} \cdot \frac{A}{A'} \cdot t \quad (5)$$

$\Delta C_0$, $h_s$, $h_c$, A, and A′ are the constants. Therefore, $D_\theta$ can be calculated through the relationship of $\Delta C_t$ and $t$.

The optimal dosage and ratio of additives were determined through the orthogonal test. The test scheme of the gas diffusion test is shown in Table 3. The gas diffusion test was conducted as per the single chamber method recommended by Taylor et al. [39–41]. The testing schematic apparatus used for this study is shown in Figure 3. The apparatus consisted of a gas diffusion chamber, an oxygen transducer (KE-25, HELM AG., Hamburg, Germany), and a data acquisition (NL-115, HELM AG., Hamburg, Germany).

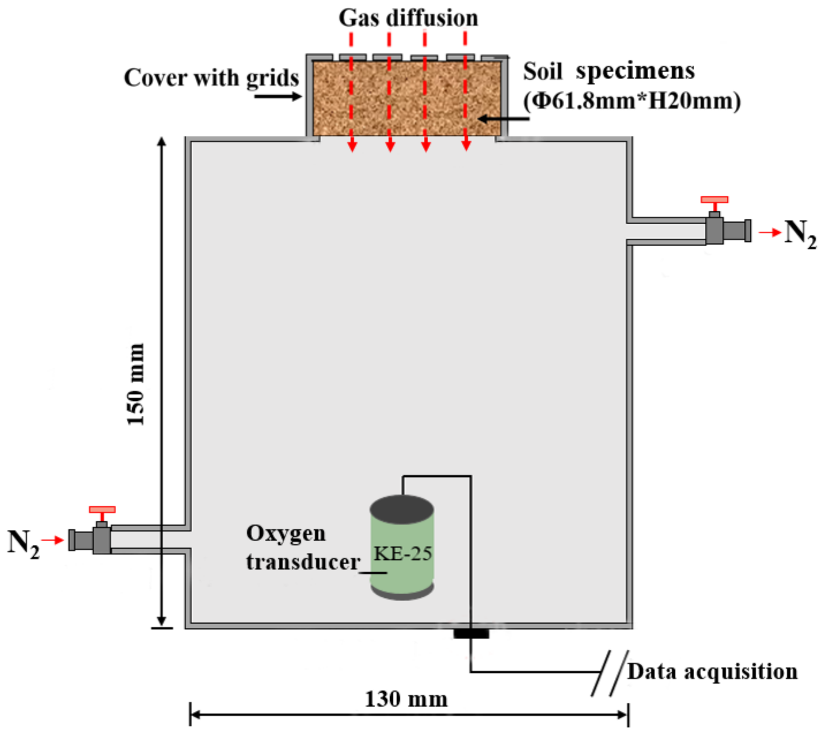


**Figure 3.** The chamber of soil gas diffusion test.

All experiments were conducted at a room temperature of 25 ± 1 °C and relative humidity of 64% ± 2% as per the following procedures: (1) The vacuum grease was applied to the inner wall of the cover (with 85% grids on the top) and outer wall of chamber top for lubrication and sealing. Then the prepared specimens were placed on the top of the chamber, and capped with the cover. (2) The inlet valve connected with the nitrogen cylinder and outlet valve was opened. It was deemed that the air in the chamber was discharged completely by nitrogen until oxygen concentration in the chamber decreased to 0.3–0.6%. Then, the inlet and outlet valves were closed after continuing to supply nitrogen for 10–15 s. (3) The data acquisition and oxygen transducer were used to automatically collect and record the oxygen concentration ($C_t$) in the chamber per 5 min until the oxygen concentration in the chamber was the same as the atmosphere ($C_0$) and reached the stable state ($C_t = C_0$). Combining the $C_t$ and $C_0$ obtained from the above, the gas diffusion coefficient $D_\theta$ was calculated based on Equation (5).

*2.4. Flexible-Wall Hydraulic Conductivity Test*

The unamended, attapulgite-amended, diatomite-amended, and dual-additives (attapulgite 4% and diatomite 1%)-amended compacted clay were prepared with moisture content of 30% and additives dosage of 5%. The degree of compaction was set as 85%. The specimens of 50 mm in diameter and 50 mm in height were prepared, assembled in a flexible-wall permeameter, and saturated using deaired tap water. Hydraulic conductivity test was conducted in the permeameter using the constant head method as per ASTM D 5084 [42]. All hydraulic conductivity tests in the study were conducted under hydraulic gradients (*i*) of 40 and effective confining stress of 36.7 kPa calculated by Equation (6) as follows [43–45].

$$\sigma_c{}' = \sigma_3 - \frac{1}{3}(p_2 + 2p_1) \tag{6}$$

where $\sigma_c{}'$= average effective confining stress; $\sigma_3$ = cell pressure (50 kPa in this study); $p_1$ = bottom seepage pressure (20 kPa in this study); $p_2$ = top seepage pressure (0 kPa in this study).

### 2.5. Scanning Electron Microscopy (SEM) and Mercury Intrusion Porosimetry (MIP) Tests

Image analyses using SEM (SIGMA 500, ZEISS-Tech, Jena, Germany) and pore size distribution using MIP (AutoPore V 9620, Micromeritics Instrument Corporation, Atlanta, America) were performed on the amended compacted clay specimens to evaluate the microstructural-amended mechanism. First, the attapulgite-amended, diatomite-amended, dual-additives-amended, and unamended compacted clay specimens were cut into 1 $cm^3$ pieces, the dosages of additives were all 5% (dry weight basis), and the ratio of dual-additives was 4 (dry weight of attapulgite 4% to dry weight of diatomite 1%). Then, the SEM and MIP specimens were frozen using liquid nitrogen for 5 min at a temperature of −120 °C. Sublimation of water was conducted at a temperature of −80 °C for 24 h in a vacuum freeze-drying unit at −18 N (Nanjing Xianou Instruments Manufacture Co., Ltd., Nanjing, China). After freeze-drying, the frozen SEM specimens were cut into small blocks with a natural fracture surface area of approximately 0.25 $cm^2$, and these blocks were coated with a thin gold layer and then subjected to SEM analyses. The freeze-dried MIP specimens were subjected to MIP analyses in compliance with ASTM D 4404-18.

### 2.6. BET Specific Surface Area Test Method (BET) and Thermogravimetric Analysis (TGA)

To evaluate the mechanisms of additives treatment, BET and TGA (DSC200F3, NETZSCH-Gerätebau GmbH, Germany), analyses were conducted on attapulgite-amended, diatomite-amended, dual-additives-amended, and unamended compacted clay specimens. The specimens were prepared according to the procedures as follows. First, the attapulgite-amended, diatomite-amended, dual-additives-amended, and unamended clay powders were mixed thoroughly to prepare the dry mixture. The dosages of additives were all designed as 5% (dry weight basis) and the ratio of dual-additives was 4 (dry weight of attapulgite 4% to dry weight of diatomite 1%). Then, the powder mixtures were frozen using liquid nitrogen for 5 min at a temperature of −120 °C. Sublimation of water was conducted at a temperature of −80 °C for 24 h in a vacuum freeze-drying unit at −18 N (Nanjing Xianou Instruments Manufacture Co., Ltd., Nanjing, China). Then, the specimens were subjected to BET and TG analyses, respectively.

## 3. Results and Discussion

### 3.1. Liquid–Plastic Limit and Moisture Retention Tests Results

Figure 4 presents the plasticity chart of the clay amended by additives with different dosages and ratios. The dosage of dual-additives-amended compacted clay was 5%. As the dosage of attapulgite increased from 0% to 10%, the plastic limit of attapulgite-amended specimens increased from 28% to 41%, and the liquid limit increased from 54% to 74%. Its liquid limit increased by 36% compared with unamended clay. With the dosage of diatomite increasing from 0% to 10%, the plastic limit of clay increased from 28% to 29%, and the liquid limit increased from 54% to 57%. Its liquid limit increased by about 5% compared with the unamended clay. The effect of diatomite on the liquid limit of amended compacted clay was not significant. When the mass ratio of attapulgite to diatomite was 0.25, the plastic limit of the dual-additives-amended compacted clay decreased from 32% to 30%, and the liquid limit decreased from 64% to 60% compared with the mass ratio of 4. The decreasing ranges of plastic limit and liquid limit were 9% and 6% respectively. When the dosage is 5%, the liquid limit of the compacted clay amended by attapulgite and dual-additives (ratio of 4) were 62% and 64% respectively.

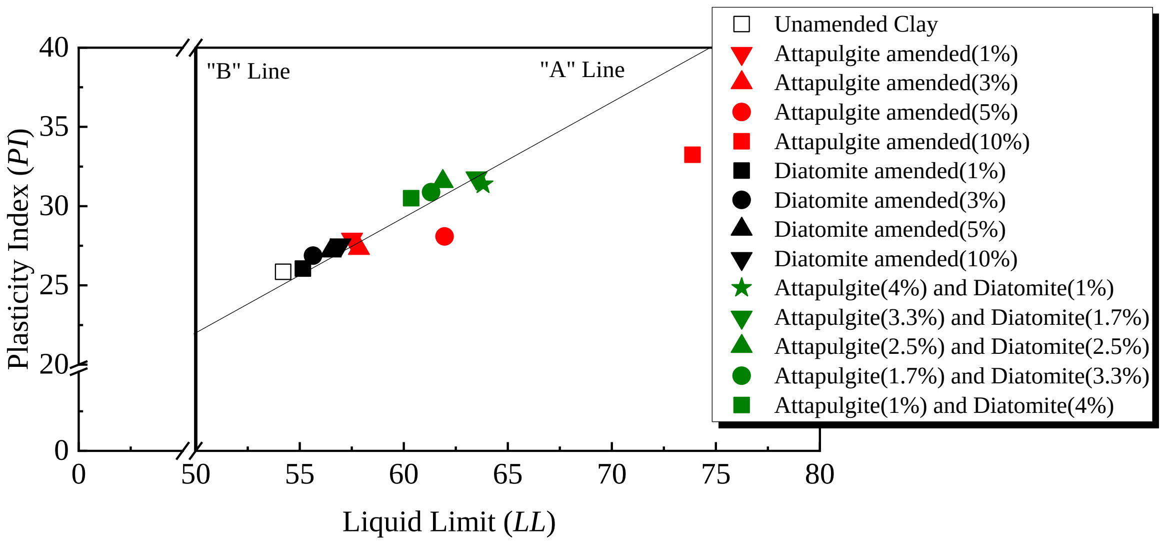


**Figure 4.** The plasticity chart of the clay amended by additives with different dosages and ratios.

Figure 5 shows how moisture retention percent varies with the dosage of additives. In general, the moisture retention percent increases with the dosage of the attapulgite increasing, while the dosage of diatomite has little effect on its moisture retention percent. The moisture retention percent with the 10% dosage of attapulgite was similar to 5%. When the attapulgite dosage was 5%, the moisture retention percent was about 66% higher than that of unamended clay. Attapulgite could effectively increase the liquid limit of clay and enhance its moisture retention capacity. When the diatomite dosage was 5%, the moisture retention percent was the largest, which was 7% higher than that of unamended clay. Therefore, the dosage of attapulgite and diatomite was found to be 5% considering the cost.

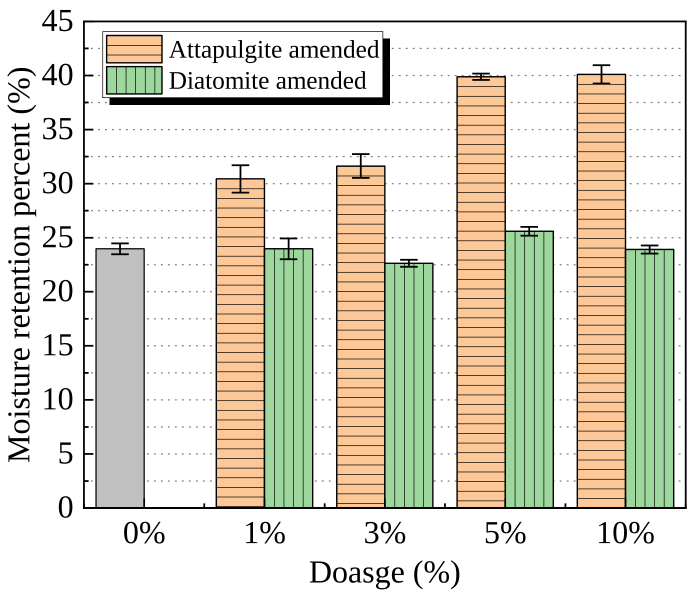


**Figure 5.** The moisture retention percent with different dosages of attapulgite and diatomite.

Figure 6 presents the variation of moisture retention percent of the dual-additives-amended clay with the ratio of attapulgite to diatomite. The moisture retention capacity of dual-additives-amended compacted clay was the best when the dry weight of attapulgite to the dry weight of diatomite was 4, which was 82% higher than that of unamended clay. It shows that the dual-additives have a great effect on enhancing the moisture retention capacity of amended compacted clay. The liquid limit of compacted clay amended by dual-additives was 3% higher than attapulgite with the dosage of 5%. The moisture retention percent of compacted clay amended by dual-additives (ratio of 4) was 9% higher than attapulgite with the dosage of 5%. Therefore, the increase in the liquid limit of compacted clay amended by additives is one of the reasons for the improvement of its moisture retention capacity.

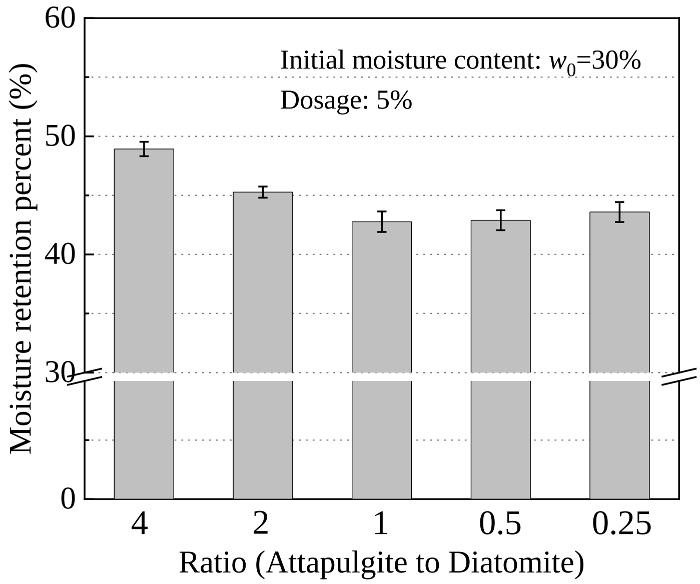


**Figure 6.** The moisture retention percent with different ratios of attapulgite to diatomite.

The results showed that the attapulgite could greatly increase the moisture retention percent, whereas the diatomite has a limited effect. It is attributed to the molecule's structure [46–48]. There are a lot of pores in the crystal of attapulgite, which could adsorb most cations, water molecules, and organic molecules of a certain size with the Van der Waals Forces, similar to a "zeolite molecular sieve". At the same time, the crystalline water molecules combined with $Mg^{2+}$ at the edge could form a hydrogen bond, which belonged to the synergistic effect of physical adsorption and chemical adsorption. Whereas, the adsorption mechanism of diatomite is mainly chemical adsorption [49–51]. It could adsorb water molecules due to the hydrogen bonds which are combined with the water molecules and the hydroxyl belonged to the Silanol group and silanediol group. However, it has a limited effect on enhancing the moisture retention percent of clay due to the weak chemical adsorption. Therefore, attapulgite could be screened as an additive to enhance the moisture retention capacity.

### *3.2. Gas Diffusion Test Results*

The results of the gas diffusion test of the compacted clay amended by attapulgite or diatomite are shown in Figure 7. The oxygen concentration in the diffusion chamber increased with the time of all dosages. At which time the oxygen concentrations inside and outside the chamber were the same, it reached equilibrium. Figure 7 presents that the $D_\theta$ decreased with the increase of attapulgite dosage and its gas barrier performance gradually improved. With the increase in dosage of diatomite, the diffusion rate of oxygen decreased. It shows that diatomite has a good effect on gas barrier performance. It also indicates that diatomite could reduce the $D_\theta$ of clay better.

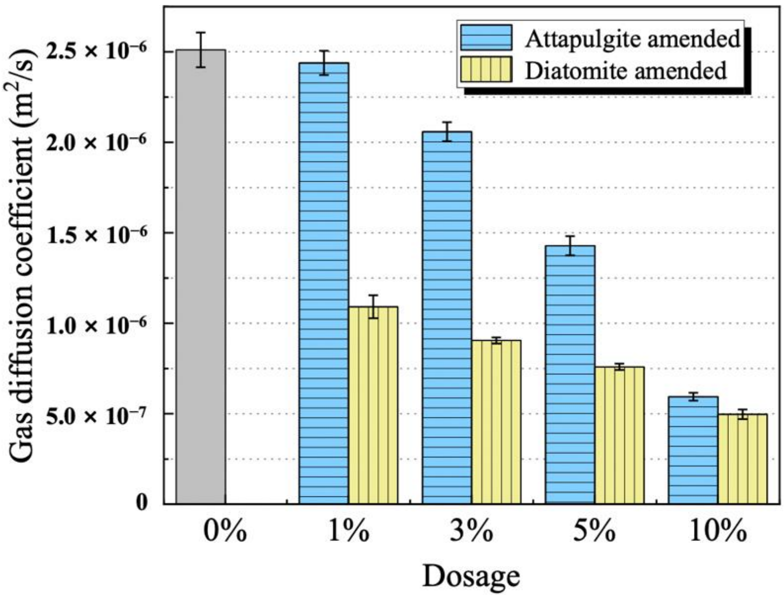


**Figure 7.** The gas diffusion coefficient with different dosages of attapulgite and diatomite.

The results of the gas diffusion test with different ratios of dual-additives are shown in Figure 8. The initial moisture content was 30% and the dosage of dual-additives was 5% of all the specimens. Among that, the $D_\theta$ of the amended clay was the lowest at $4.4 \times 10^{-7}$ m$^2$/s when the ratio was 1. After considering the economic cost, the dosage of diatomite should be reduced as much as possible. Therefore, it is suggested that the mass ratio of attapulgite to diatomite be 4, the dosage 5%, and the $D_\theta$ of the amended compacted clay $8.5 \times 10^{-7}$ m$^2$/s, reduced by about 42% compared with the unamended clay.

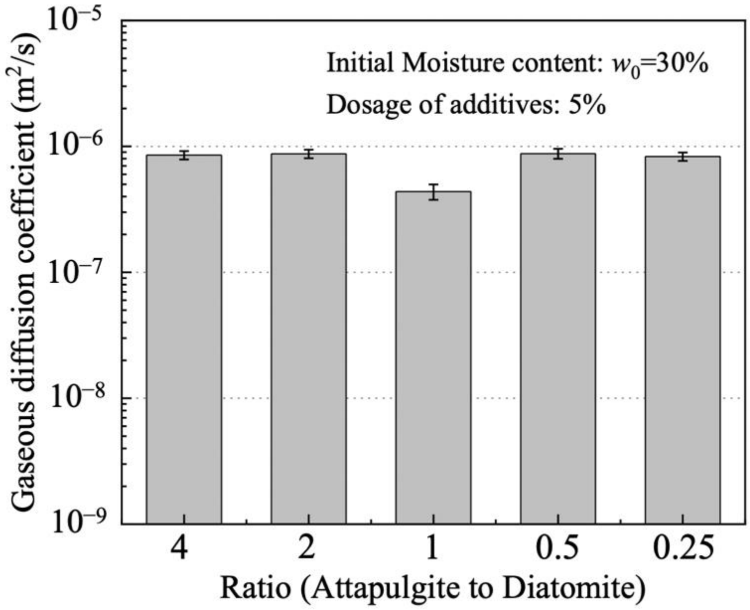


**Figure 8.** The effect of ratios of additives on the gas diffusion coefficient.

Comparing the gas diffusion test results of the clay amended by attapulgite and diatomite, it can be obtained that the effect of diatomite on the gas barrier performance of the clay is more obvious compared with that of attapulgite, which can be attributed to those crystal structures. Nevertheless, the attapulgite crystals are chain structures or fibrous structures [48], meaning the gas could still migrate through the gap of fibrous or chain structure between the crystals after mixing and compaction. While diatomite, as a porous layered siliceous rock of biological genesis, is composed of diatom wall shells, which are distributed with microporous structure [49–51]. There are few and complex channels for gas migration owing to its wall shells. Therefore, diatomite could be screened as one of the additives to improve the gas barrier performance of amended compacted clay.

In conclusion, it is apparent that the optimal dosage of dual-additives was determined to be 5% and the mass ratio of attapulgite to diatomite 4, based on the experimental results of moisture retention percent and gas diffusion coefficient. In addition, the economic cost is also a factor to be considered.

### 3.3. Flexible-Wall Hydraulic Conductivity Test Results

Figure 9 shows the results of hydraulic conductivity of amended compacted clay. During permeation with tap water, the $k$ of the unamended, attapulgite amended, diatomite amended, and dual-additives-amended compacted clay were $8.3 \times 10^{-9}$ m/s, $6.3 \times 10^{-9}$ m/s, $7.4 \times 10^{-9}$ m/s, and $5.9 \times 10^{-9}$ m/s, respectively. Importantly, the $k$ of compacted clay amended by attapulgite, diatomite, and dual-additives were lower than unamended compacted clay, which decreased by 25%, 11%, and 29%, respectively. These results indicate that the dual-additives-amended clay possessed better hydraulic performance than unamended clay.

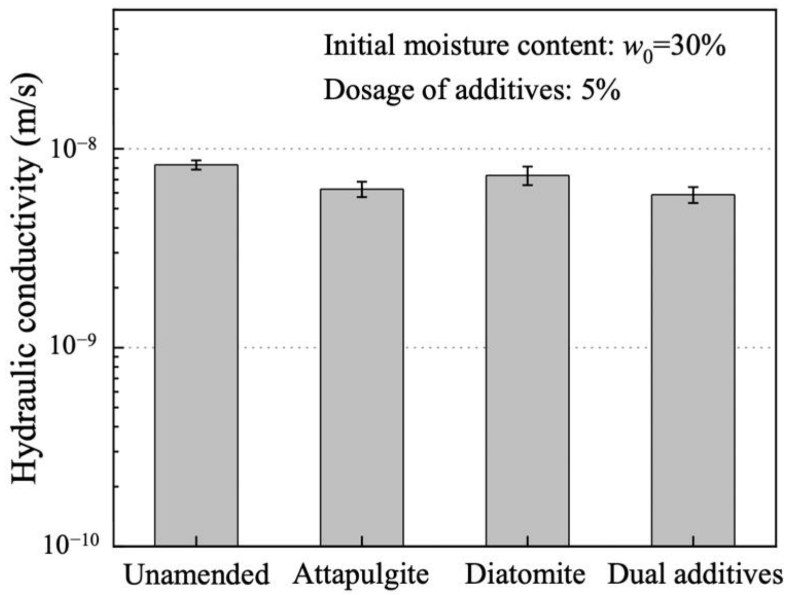


**Figure 9.** The flexible wall penetration test results of amended compacted clay.

### 3.4. SEM, BET, MIP, and TGA Tests Results

SEM images for the compacted clay specimens (a) Unamended; (b) Attapulgite-amended; (c) Diatomite-amended; and (d) Dual-additives-amended are shown in Figure 10. It is seen from Figure 10a that the flaky, unamended compacted clay particles polymerize to form agglomerates. There are gaps between adjacent agglomerates for gas and water molecules to pass through. Figure 10b shows that the acicular attapulgite particles attached to the surface of the clay and filled the gaps, which reduced the gaps between clay particles and increased the water retention percent. Figure 10c presents that the size of diatomite particles with micropores was larger than clay particles. The pores between the clay particles decreased, and the micropores on the surface of the diatomite made the gas migration path more complex. However, the microporous structure was larger than those of "zeolite molecular sieve", which had a limited effect on moisture molecules adsorption. Therefore, it had a limited effect on the enhancement of moisture retention performance. Figure 10d shows that the dual-additives filled and decreased the pores between clay particles and the micropores structure made the gas migration more complex and difficult.

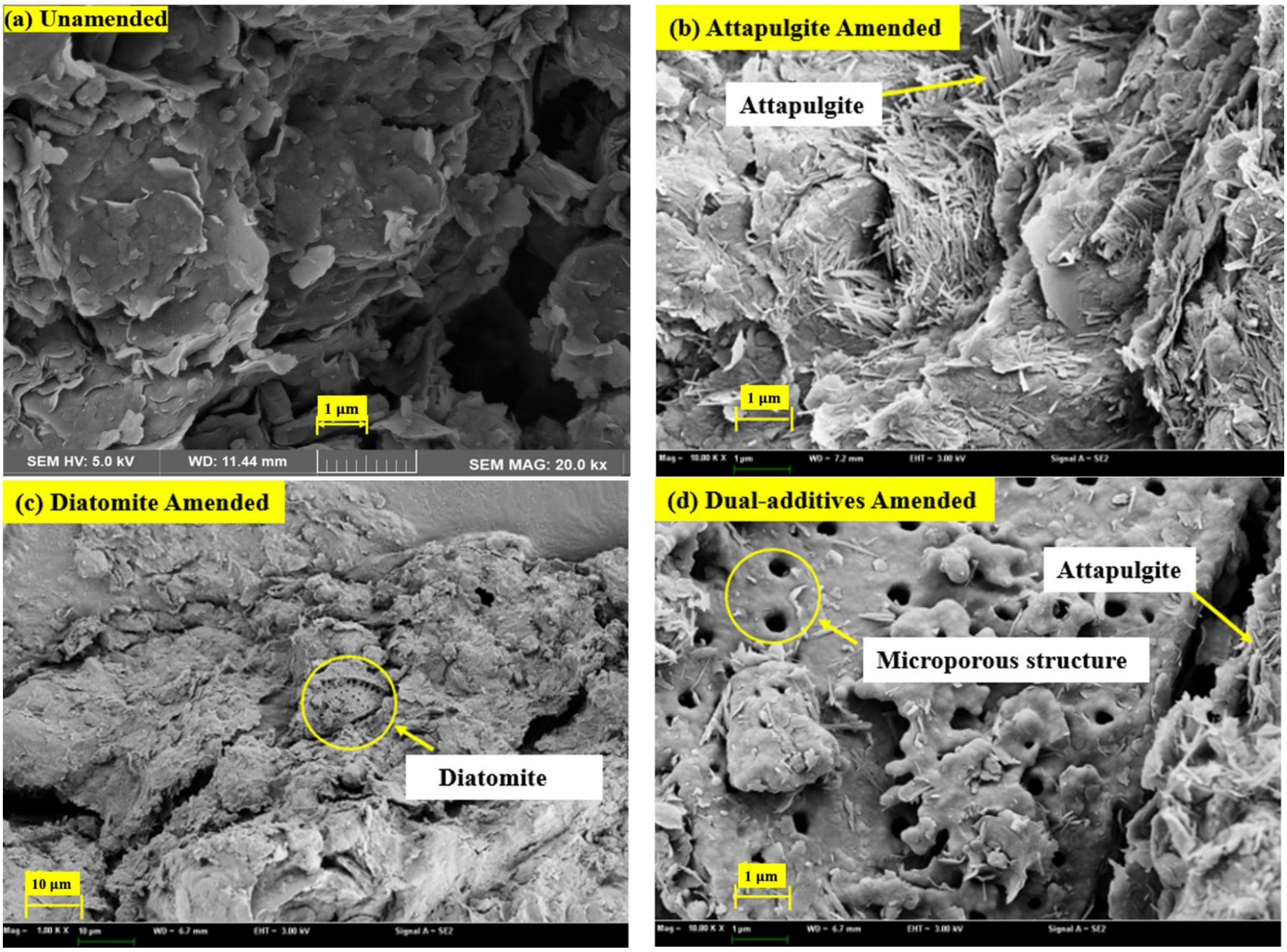


**Figure 10.** SEM images of compacted clay specimens.

Figure 11 shows the cumulative intruded pore volume and incremental intruded pore volume vs. pore size diameter (PSD) of amended compacted clay specimens with different additives (dosage 5%). The distribution is shown for a diameter range of 3 nm to 425 µm and a pressure range of 0.1 pasi to 61,000 pasi. The average PSD of specimens amended by dual-additives, attapulgite, diatomite, and unamended were 30.6, 31.19, 35.02, and 47.28 nm respectively. Porosities were 19.4%, 21.5%, 27.2%, and 47.3% respectively. The average PSD and porosity of dual-additives-amended compacted clay decreased by 55% and 144% respectively compared with unamended ones. Figure 11a presents that the cumulative intruded pore volume of all amended specimens was lower than unamended ones, regardless of PSD. The cumulative intruded pore volume of dual-additives-amended was the lowest, which decreased by 60% at PSD of 5 nm compared with unamended. It illustrates that the dual-additives filled the gaps and pores of compacted clay significantly. Figure 11b shows that the incremental intruded pore volume of unamended compacted clay increased significantly at a PSD of 100 nm. The peak of curves of amended compacted clay were in the range of 5–100 nm, especially at 15 and 40 nm. The incremental intruded pore volume of all specimens was almost zero in the range of 500–100,000 nm. It indicates that almost all of the pores in amended compacted clay had a diameter range of 5–500 nm. Therefore, the dual-additives could enhance moisture retention and gas barrier performance by decreasing the gaps and pores of compacted clay.

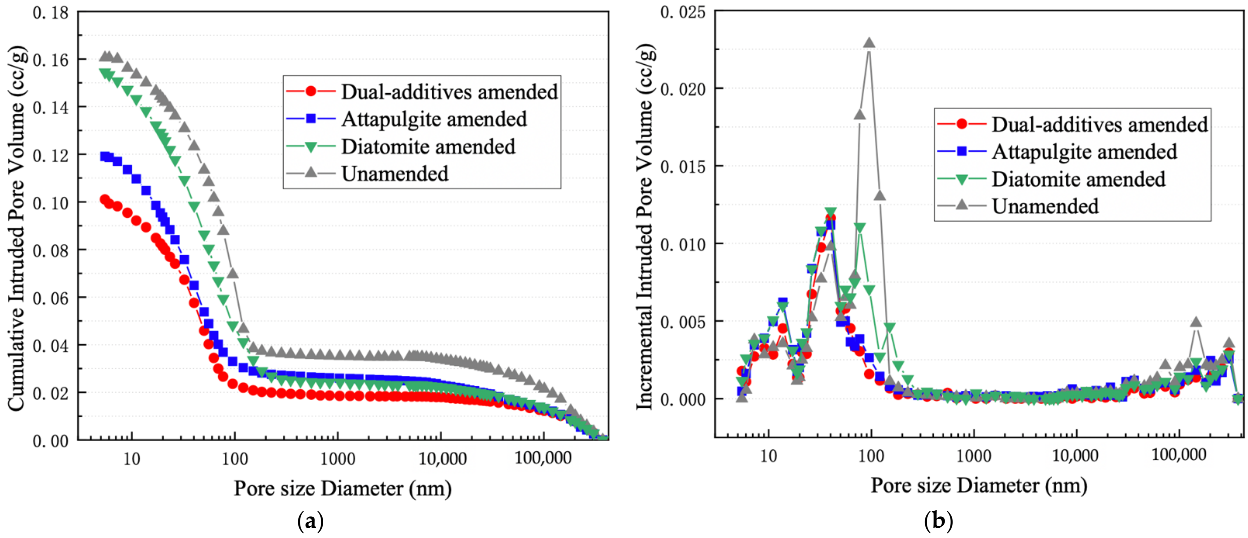


**Figure 11.** MIP results of amended compacted clay specimens: (**a**) cumulative intruded pore volume vs. pore size diameter; and (**b**) incremental intruded pore volume.

The BET test results of clay powder amended by different additives are shown in Figure 12. The PSDs of less than 2 nm, 2–50 nm, and larger than 50 nm were defined as microporous, mesoporous, and macroporous respectively. It is seen that the microporous amount of amended clay increased significantly compared with unamended clay, and the mesoporous and microporous volume increases were not significant. The microporous volume of attapulgite-amended, diatomite-amended, and dual-additives-amended clay were 0.00721 $cm^3/g{\cdot}nm$, 0.00707 $cm^3/g{\cdot}nm$, and 0.00724 $cm^3/g{\cdot}nm$ respectively when the pore size diameter was 2 nm, increases of 9%, 7%, and 9% respectively compared with unamended clay. So, the dual-additives could enhance the moisture retention performance of compacted clay. The specific surface area and Density Functional Theory (DFT) pore distribution results are presented in Table 4. It was seen that the specific surface area of clay amended by additives increased 13–15% compared with unamended clay. The volume of microporous and mesoporous attapulgite and dual-additives-amended clay increased significantly. Therefore, the dual-additives decreased the microporous size diameter of clay powder and increased its specific surface area.

**Table 4.** The BET test results.

| Specimens | Dosage | Ratio (Attapulgite to Diatomite) | Specific Surface Area ($m^2/g$) | DFT Pore Distribution ($cm^3/g$) | | Average Microporous Size Diameter (nm) |
|---|---|---|---|---|---|---|
| | | | | Less than 1.863 nm | Less than 19.577 nm | |
| Unamended | - | - | 43.5843 | 0.01119 | 0.05508 | 0.7847 |
| Attapulgite-amended | 5% | - | 49.7271 | 0.01284 | 0.07191 | 0.7829 |
| Diatomite-amended | 5% | - | 45.4255 | 0.01201 | 0.05729 | 0.7803 |
| Dual-additives-amended | 5% | 4 | 49.3243 | 0.01284 | 0.06779 | 0.7811 |

The TGA test results of clay amended by different additives are shown in Figure 13. The water in the clay was classified into tightly bound water (TBW) connected with clay minerals by hydrogen bond, loosely bound water (LBW) connected with clay minerals by molecular force [52,53], and free water; the limit of water decomposition temperature was 120~230 °C, 75~120 °C, and 25~75 °C respectively [54]. The DTG curve was obtained from the differentiation of the TG curve. Each minimum point at the valley on the DTG curve represents the water decomposition point. Figure 13a shows that the temperature limits of TBW, LBW, and free water of unamended clay were 29.4 °C, 101.55 °C, and 184.41 °C respectively. The LBW temperature limit of attapulgite-amended clay was 106.68 °C, an increased of 5.05% compared with unamended clay, and its TBW temperature limit was 210.46 °C, an increase of 14%. The LBW temperature limit of diatomite-amended clay was

105.10 °C, an increase of 3.5%, and that of dual-additives-amended clay increased by 8.9%. The TBW and free water have no relationship with the moisture retention performance of clay. The LBW is double-diffuse layers (DDLs) of clay minerals [55,56], which is the critical factor in the moisture retention performance of clay. Figures 4,5 and 13, present that the trend of the temperature limit of clay amended by different additives is consistent with the results of moisture retention percent and liquid limit. It illustrates that the moisture retention percent of amended clay increases with the increasing the temperature limit of LBW. That is attributed to the fact that the thermal energy required to lose the same amount of LBW is greater with the increasing temperature limit; therefore, its moisture retention performance is enhanced at the same temperature (60 °C).

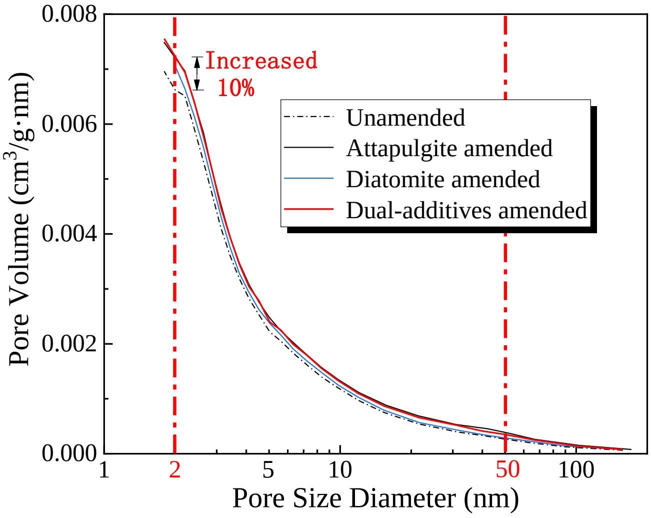


**Figure 12.** BET tests results of clay specimens amended by attapulgite, diatomite, dual-additives, and unamended.

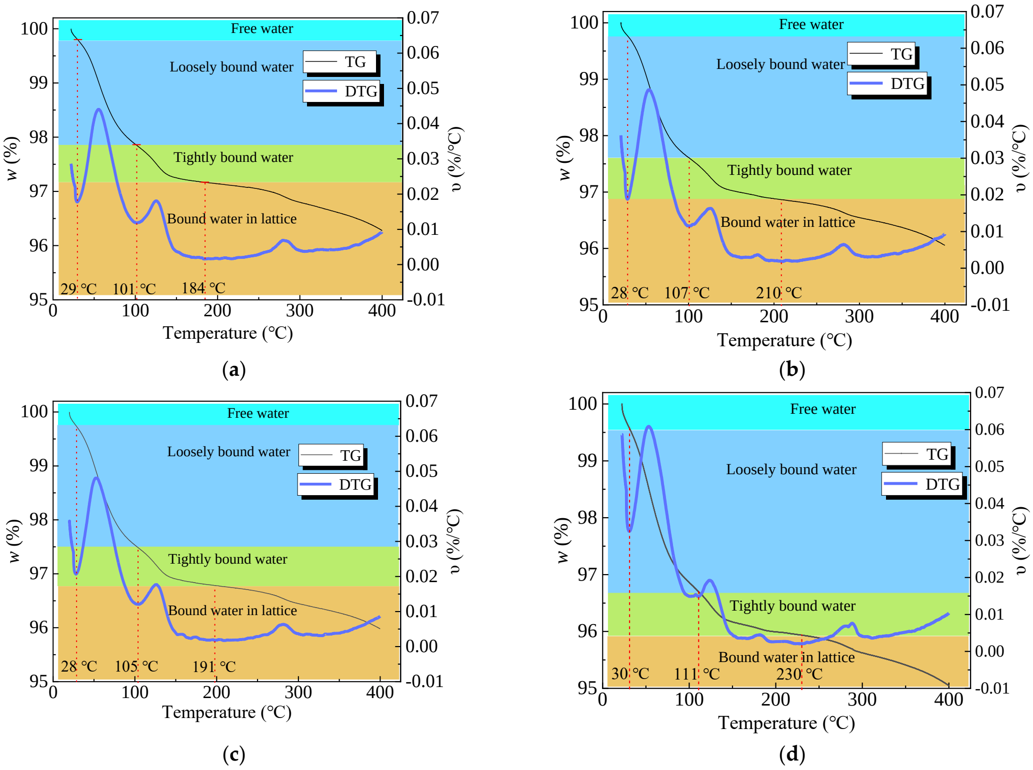


**Figure 13.** TG tests results of specimens: (**a**) Unamended; (**b**) Attapulgite-amended; (**c**) Diatomite-amended; and (**d**) Dual-additives-amended.

## 4. Conclusions

The optimum dosage and ratio of additives for amending compacted clay were screened and determined through moisture retention and gas diffusion test. The principal reason for the enhancement of its moisture retention capacity was investigated by the liquid–plastic limit test. Subsequently, the hydraulic performance of the compacted clay amended by additives and unamended was conducted. Based on the results, the following conclusions can be drawn:

1. The attapulgite could enhance the moisture retention performance of the clay, but its effect on gas barrier performance was limited. When its dosage was 5%, its moisture retention percent was 66% higher than that of unamended clay. The enhancement mechanism behind the phenomenon is attributed to increasing the liquid limit of clay;
2. The diatomite could effectively decrease the gas diffusion coefficient of clay, while it had a limited effect on the moisture retention performance. As its dosage was 5%, the moisture retention percent of clay only increased by 7%;
3. Considering the moisture retention capacity, gas barrier performance, and cost, the optimal dosage of dual-additives was targeted to be 5%, and the optimal ratio of attapulgite to diatomite was 4. The moisture retention percent of the dual-additives-amended compacted clay increased by 82%, and the gas diffusion coefficient decreased by 42% compared with unamended clay. The $k$ of enhanced compacted clay amended by attapulgite and dual-additives was $6.3 \times 10^{-9}$ m/s and $5.9 \times 10^{-9}$ m/s respectively, decreases of 25% and 29% compared with the unamended clay;
4. The SEM and MIP analyses presented that dual-additives effectively filled the intergranular pores of the amended clay and micropore structure increased the gas migration path. The BET test results showed that dual-additives increased the amount of microporous to enhance the moisture retention performance of amended clay. Meanwhile, the dual-additives increased the specific surface area and decreased the average PSD. The TGA results demonstrated that dual-additives increased the temperature limit of loosely bound water to enhance the moisture retention performance of amended clay.

**Author Contributions:** Conceptualization, M.W., J.W. and Y.D.; methodology, M.W., Y.D. and J.W.; software, M.W.; validation, M.W. and N.J.; formal analysis, M.W. and J.W.; investigation, M.W., J.W. and H.Z.; resources, M.W.; data curation, M.W. and J.W.; writing—original draft preparation, M.W., J.W., H.Z. and W.X.; writing—review and editing, M.W., Y.D., H.Z. and N.J.; visualization, M.W.; supervision, M.W., Y.D. and W.X.; project administration, Y.D.; funding acquisition, Y.D. All authors have read and agreed to the published version of the manuscript.

**Funding:** Financial support for this project was provided by the National Key R&D Program of China (Grant No. 2018YFC1803100), the National Natural Science Foundation of China (Grant Nos. 41877248, 42177133, and 41902276).

**Data Availability Statement:** Some or all data, models, or code that support the findings of this study are available from the corresponding author upon reasonable request.

**Conflicts of Interest:** The authors declare that they have no known competing financial interests or personal relationships that could have appeared to influence the work reported in this paper.

## References

1. Chen, Z.; Kamchoom, V.; Chen, R. Landfill gas emission through compacted clay considering effects of crack pathway and intensity. *Waste Manag.* **2022**, *143*, 215–222. [PubMed]
2. Albright, W.H.; Benson, C.H.; Gee, G.W.; Abichou, T.; McDonald, E.V.; Tyler, S.W.; Rock, S.A. Field performance of a compacted clay landfill final cover at a humid site. *J. Geotech. Geoenviron. Eng.* **2006**, *132*, 1393–1403.
3. Ng, C.W.W.; Chen, Z.K.; Coo, J.L.; Chen, R.; Zhou, C. Gas breakthrough and emission through unsaturated compacted clay in landfill final cover. *Waste Manag.* **2015**, *44*, 155–163. [PubMed]
4. Mahmoodlu, M.G.; Hassanizadeh, S.M.; Hartog, N.; Raoof, A.; van Genuchten, M.T. Evaluation of a horizontal permeable reactive barrier for preventing upward diffusion of volatile organic compounds through the unsaturated zone. *J. Environ. Manag.* **2015**, *163*, 204–213.

5. Verginelli, I.; Capobianco, O.; Hartog, N.; Baciocchi, R. Analytical model for the design of in situ horizontal permeable reactive barriers (HPRBs) for the mitigation of chlorinated solvent vapors in the unsaturated zone. *J. Contam. Hydrol.* **2017**, *197*, 50–61.
6. Rowe, R.K.; Brachman, R.W.I. Assessment of equivalence of composite liners. *Geosynth. Int.* **2004**, *11*, 273–286.
7. Hewitt, P.J.; Philip, L.K. Problems of clay desiccation in composite lining systems. *Eng. Geol.* **1999**, *53*, 107–113.
8. Omidi, G.H.; Thomas, J.C.; Brown, K.W. Effect of desiccation cracking on the hydraulic conductivity of a compacted clay liner. *Water Air Soil Pollut.* **1996**, *89*, 91–103.
9. Julina, M.; Thyagaraj, T. Combined effects of wet-dry cycles and interacting fluid on desiccation cracks and hydraulic conductivity of compacted clay. *Eng. Geol.* **2020**, *267*, 105505.
10. Aldaeef, A.A.; Rayhani, M.T. Hydraulic performance of compacted clay liners under simulated daily thermal cycles. *J. Environ. Manag.* **2015**, *162*, 171–178.
11. Tang, C.S.; Shi, B.; Liu, C.; Suo, W.B.; Gao, L. Experimental characterization of shrinkage and desiccation cracking in thin clay layer. *Appl. Clay Sci.* **2011**, *52*, 69–77.
12. Amarasiri, A.L.; Kodikara, J.K.; Costa, S. Numerical modelling of desiccation cracking. *Int. J. Numer. Anal. Methods Geomech.* **2011**, *35*, 82–96.
13. Kodikara, J.K.; Choi, X. A simplified analytical model for desiccation cracking of clay layers in laboratory tests. In *Unsaturated Soils, Proceedings of the UNSAT 2006 Conference, Carefree, AZ, USA, 2–6 April 2006*; Miller, G.A., Zapata, C.E., Houston, S.L., Fredlund, D.G., Eds.; ASCE Geotechnical Special Publication: Carefree, AZ, USA, 2006; Volume 2, pp. 2558–2567.
14. Albrecht, B.A.; Benson, C.H. Effect of desiccation on compacted natural clays. *J. Geotech. Geoenviron. Eng.* **2001**, *127*, 67–75.
15. Kabiri, K.; Omidian, H.; Zohuriaan-Mehr, M.J.; Doroudiani, S. Superabsorbent hydrogel composites and nanocomposites: A review. *Polym. Compos.* **2011**, *32*, 277–289.
16. Farrell, C.; Ang, X.Q.; Rayner, J.P. Water-retention additives increase plant available water in green roof substrates. *Ecol. Eng.* **2013**, *52*, 112–118.
17. Polman, E.M.; Gruter, G.J.M.; Parsons, J.R.; Tietema, A. Comparison of the aerobic biodegradation of biopolymers and the corresponding bioplastics: A review. *Sci. Total Environ.* **2021**, *753*, 141953.
18. Florez, C.; Restrepo-Baena, O.; Tobon, J.I. Effects of calcination and milling pre-treatments on natural zeolites as a supplementary cementitious material. *Constr. Build. Mater.* **2021**, *310*, 125220.
19. Conant, B.H.; Gillham, R.W.; Mendoza, C.A. Vapor transport of trichloroethylene in the unsaturated zone: Field and numerical modeling investigations. *Water Resour. Res.* **1996**, *32*, 9–22.
20. You, K.; Zhan, H. Comparisons of diffusive and advective fluxes of gas phase volatile organic compounds (VOCs) in unsaturated zones under natural conditions. *Adv. Water Resour.* **2013**, *52*, 221–231.
21. Li, H.; Jiao, J.J. One-dimensional airflow in unsaturated zone induced by periodic water table fluctuation. *Water Resour. Res.* **2005**, *41*, 1–10. [CrossRef]
22. Li, J.; Zhan, H.; Huang, G.; You, K. Tide-induced airflow in a two-layered coastal land with atmospheric pressure fluctuations. *Adv. Water Resour.* **2011**, *34*, 649–658.
23. You, K.; Zhan, H. Can atmospheric pressure and water table fluctuations be neglected in soil vapor extraction? *Adv. Water Resour.* **2012**, *35*, 41–54.
24. Jiao, J.J.; Li, H. Breathing of coastal vadose zone induced by sea level fluctuations. *Geophys. Res. Lett.* **2004**, *31*, L11502. [CrossRef]
25. Guo, H.P.; Jiao, J.J. Numerical study of airflow in the unsaturated zone induced by sea tides. *Water Resour. Res.* **2008**, *44*, W06402. [CrossRef]
26. You, K.; Zhan, H.; Li, J. A new solution and data analysis for gas flow to a barometric pumping well. *Adv. Water Resour.* **2010**, *33*, 1444–1455.
27. You, K.; Zhan, H.; Li, J. Gas flow to a barometric pumping well in a multilayer unsaturated zone. *Water Resour. Res.* **2011**, *47*, W05522. [CrossRef]
28. Choi, J.W.; Smith, J.A. Geoenvironmental factors affecting organic vapor advection and diffusion fluxes from the unsaturated zone to the atmosphere under natural conditions. *Environ. Eng. Sci.* **2005**, *22*, 95–108.
29. Smith, J.A.; Chiou, C.T.; Kammer, J.A.; Kile, D.E. Effect of soil moisture on the sorption of trichloroethene vapor to vadose-zone soil at Picatinny Arsenal, New Jersey. *Environ. Sci. Technol.* **1990**, *24*, 676–683.
30. Batterman, S.A.; McQuown, B.C.; Murthy, P.N.; McFarland, A.R. Design and evaluation of a long-term soil gas flux sampler. *Environ. Sci. Technol.* **1992**, *26*, 709–714.
31. Rowe, R.K. Environmental Geotechnics: Past, Present and Future? In Proceedings of the 8th International Congress on Environmental Geotechnics, Hangzhou, China, 28 October–1 November 2018; Springer: Singapore, 2018.
32. *ASTM D 698*; Standard Test Methods for Laboratory Compaction Characteristics of Soil Using Standard Effort (12,400 ft-lbf/ft$^3$ (600 kN-m/m$^3$)). ASTM: West Conshohocken, PA, USA, 2012.
33. *ASTM D 4318*; Standard Test Methods for Liquid Limit, Plastic Limit, and Plasticity Index of Soils. ASTM: West Conshohocken, PA, USA, 2018b.
34. *ASTM D 854*; Standard Test Methods for Specific Gravity of Soil Solids by Water Pycnometer. ASTM: West Conshohocken, PA, USA, 2014b.
35. Sun, L.P.; Du, Y.M.; Shi, X.W.; Chen, X.; Yang, J.H.; Xu, Y.M. A new approach to chemically modified carboxymethyl chitosan and study of its moisture-absorption and moisture-retention abilities. *J. Appl. Polym. Sci.* **2006**, *102*, 1303–1309.

36. Barajas-Ledesma, R.M.; Wong, V.N.; Little, K.; Patti, A.F.; Garnier, G. Carboxylated nanocellulose superabsorbent: Biodegradation and soil water retention properties. *J. Appl. Polym. Sci.* **2022**, *139*, 51495.
37. Mi, Y.; Miao, Q.; Cui, J.; Tan, W.; Guo, Z. Novel 2-Hydroxypropyltrimethyl Ammonium Chitosan Derivatives: Synthesis, Characterization, Moisture Absorption and Retention Properties. *Molecules* **2021**, *26*, 4238. [CrossRef]
38. Wang, J.; Jin, W.; Hou, Y.; Niu, X.; Zhang, H.; Zhang, Q. Chemical composition and moisture-absorption/retention ability of polysaccharides extracted from five algae. *Int. J. Biol. Macromol.* **2013**, *57*, 26–29. [PubMed]
39. Taylor, S.A. Oxygen diffusion in porous media as a measure of soil aeration. *Soil Sci. Soc. Am. J.* **1950**, *14*, 55–61.
40. Currie, J.A. Gaseous diffusion in porous media Part 1. A non-steady state method. *Br. J. Appl. Phys.* **1960**, *11*, 314–317.
41. Su, Z.; Wu, B.; Gong, Y. Determination of gas diffusion coefficient in soils with different porosities. *Trans. Chin. Soc. Agric. Eng.* **2015**, *31*, 108–113.
42. *ASTM D5084*; Standard Test Methods for Measurement of Hydraulic Conductivity of Saturated Porous Materials Using a Flexible Wall Permeameter. ASTM: West Conshohocken, PA, USA, 2016.
43. Malusis, M.A.; McKeehan, M.D. Chemical compatibility of model soil-bentonite backfill containing multiswellable bentonite. *J. Geotech. Geoenviron. Eng.* **2013**, *139*, 189–198.
44. Bohnhoff, G.L.; Shackelford, C.D. Hydraulic conductivity of polymerized bentonite-amended backfills. *J. Geotech. Geoenviron. Eng.* **2014**, *140*, 04013028.
45. Yang, Y.L.; Reddy, K.R.; Du, Y.J.; Fan, R.D. Short-term hydraulic conductivity and consolidation properties of soil-bentonite backfills exposed to CCR-impacted groundwater. *J. Geotech. Geoenviron. Eng.* **2018**, *144*, 04018025.
46. Boudriche, L.; Calvet, R.; Hamdi, B.; Balard, H. Effect of acid treatment on surface properties evolution of attapulgite clay: An application of inverse gas chromatography. *Colloid. Surf.* **2011**, *392*, 45–54.
47. Duan, Z.; Zhao, Q.; Wang, S.; Yuan, Z.; Zhang, Y.; Li, X.; Wu, Y.; Jiang, Y.; Tai, H. Novel application of attapulgite on high performance and low-cost humidity sensors. *Sens. Actuators B Chem.* **2020**, *305*, 127534.
48. Liu, D.B.; Li, Y.; Xiao, H.F.; Xu, L.D.; Zhou, Y.Z.; Han, W.Y.; Li, H.R.; Jiang, Y.M.; Qiu, Y.S. Attapulgite Clay and Its Application in Radionuclide Treatment: A Review. *Sci. Adv. Mater.* **2018**, *10*, 1529–1542.
49. de Namor, A.F.D.; El Gamouz, A.; Frangie, S.; Martinez, V.; Valiente, L.; Webb, O.A. Turning the volume down on heavy metals using tuned diatomite. A review of diatomite and modified diatomite for the extraction of heavy metals from water. *J. Hazard. Mater.* **2012**, *241*, 14–31.
50. Sun, M.; Zou, C.; Xin, D. Pore structure evolution mechanism of cement mortar containing diatomite subjected to freeze-thaw cycles by multifractal analysis. *Cem. Concr. Compos.* **2020**, *114*, 103731.
51. Zheng, J.; Shi, J.; Ma, Q.; Dai, X.; Chen, Z. Experimental study on humidity control performance of diatomite-based building materials. *Appl. Therm. Eng.* **2017**, *114*, 450–456.
52. Li, Y.L.; Wang, T.H.; Su, L.J. Determination of bound water content of loess soils by isothermal adsorption and thermogravimetric analysis. *Soil Sci.* **2015**, *180*, 90–96.
53. Li, S.; Wang, C.; Zhang, X.; Zou, L.; Dai, Z. Classification and characterization of bound water in marine mucky silty clay. *J. Soils Sediments* **2019**, *19*, 2509–2519.
54. Wang, Y.; Lu, S.; Ren, T.; Li, B. Bound water content of air-dry soils measured by thermal analysis. *Soil Sci. Soc. Am. J.* **2011**, *75*, 481–487.
55. Fu, X.L.; Shen, S.Q.; Reddy, K.R.; Yang, Y.L.; Du, Y.J. Hydraulic Conductivity of Sand/Biopolymer-Amended Bentonite Backfills in Vertical Cutoff Walls Permeated with Lead Solutions. *J. Geotech. Geoenviron. Eng.* **2022**, *148*, 04021186.
56. Zhuang, H.; Wang, J.; Gao, Z. Anisotropic and Noncoaxial Behavior of Soft Marine Clay under Stress Path Considering the Variation of Principal Stress Direction. *Int. J. Geomech.* **2022**, *22*, 04022062.